Carbohydrate Research 344 (2009) 1734–1744

Contents lists available at ScienceDirect

Carbohydrate Research

journal homepage: www.elsevier.com/locate/carres

Single-crystal and powder X-ray diffraction and solid-state ^{13}C NMR of *p*-nitrophenyl glycopyranosides, the derivatives of D-galactose, D-glucose, and D-mannose

Tomasz Gubica [a], Andrzej Temeriusz [a,*], Katarzyna Paradowska [b], Andrzej Ostrowski [c], Paulina Klimentowska [a], Michał K. Cyrański [a]

[a] Faculty of Chemistry, University of Warsaw, Pasteura 1, PL-02093 Warsaw, Poland
[b] Department of Physical Chemistry, Faculty of Pharmacy, Medical University of Warsaw, Banacha 1, PL-02097 Warsaw, Poland
[c] Faculty of Chemistry, Warsaw University of Technology, Noakowskiego 3, PL-00664 Warsaw, Poland

ARTICLE INFO

Article history:
Received 3 March 2009
Received in revised form 20 May 2009
Accepted 25 May 2009
Available online 2 June 2009

Keywords:
Crystal structure
Single-crystal X-ray diffraction
Powder X-ray diffraction
Solid-state NMR
Nitrophenyl glycopyranosides

ABSTRACT

The X-ray diffraction patterns, ^{13}C CP MAS NMR spectra, and powder X-ray diffraction analyses were obtained for selected *p*-nitrophenyl glycosides: α- and β-D-galactopyranosides (**1** and **2**), α- and β-D-glucopyranosides (**3** and **4**), and α- and β-D-mannopyranosides (**5** and **6**). In X-ray diffraction analysis of **1** and **2**, characteristic shortening and lengthening of selected bonds were observed in the molecules of **1** due to anomeric effect, and in the crystal lattice of **1** and **2**, hydrogen bonds of complex network were detected. In the crystal asymmetric unit of **1** there were two independent molecules, whereas in **2** there was one molecule. For **1** and **3**–**6** the number of resonances in solid-state ^{13}C NMR spectra exceeded the number of the carbon atoms in the molecules, while for **2** there were distinct singlet resonances in its solid-state NMR spectrum. Furthermore, the powder X-ray diffraction (PXRD) performed for **1**–**3** and **5** revealed that **1**, **3**, and **5** existed as single polymorphs proving that the doublets observed in appropriate solid-state NMR spectra were connected with two non-equivalent molecules in the crystal asymmetric unit. On the other hand **2** existed as a mixture of two polymorphs, one of them was almost in agreement with the calculated pattern obtained from XRD (the difference in volumes of the unit cells), and the subsequent unknown polymorph existed in small amounts and therefore it was not observed in solid-state NMR measurements.

1. Introduction

Glycosides are a group of natural compounds widely spread in both flora and fauna.[1] Therefore, glycosidases, the enzymes that catalyze the decomposition of corresponding glycosides are a subject of intense investigations regarding their kinetics and mechanism of action.[2–16]

The first step in these investigations is the isolation of glycosidases from natural materials, often using the affinity chromatography. In this technique, specific ligands, covalently bound to the supporting, stationary phase which can recognize specific natural substances are needed. Such ligands which can be used for isolating glycosidases are the *p*-aminophenyl glycosides.[17] The simplest precursors of *p*-aminophenyl glycosides are their *p*-nitrophenyl counterparts, which can be easily converted into the corresponding *p*-aminophenyl derivatives.[18–20] The *p*-nitrophenyl glycosides are also used as markers in the investigations of the kinetics of glycosidases,[21–26] since during enzymatic decomposition the free aglycon, that is, *p*-nitrophenol, is released and therefore the changes of absorbance in UV–vis spectrum can be observed.

The important applications of *p*-nitrophenyl glycosides listed above prompted us to investigate their structure using not only the X-ray diffraction, but also the solid-state ^{13}C NMR techniques (Table 1). These techniques are complementary. Single-crystal X-ray diffraction (XRD) measurements can provide the information about the number of molecules in the independent unit cell of the appropriate monocrystals, while the powder X-ray diffraction (PXRD) experiments deliver information about the number of crystalline forms in the samples, and can associate the appropriate polymorph with the data obtained from XRD. Similarly to powder X-ray diffraction (PXRD), the solid-state ^{13}C NMR techniques relate to macroscopic samples, not only to selected monocrystals, and therefore they can reveal the number of magnetically unequal molecules in these samples providing the additional information about the structure of the selected *p*-nitrophenyl glycosides. As discussed by Harris,[27] solid-state NMR has been successfully applied to the studies of organic molecules in a variety of chemical systems,

* Corresponding author. Tel.: +48 22 822 2325; fax: +48 22 822 5996.
E-mail address: atemer@chem.uw.edu.pl (A. Temeriusz).

0008-6215/$ - see front matter © 2009 Elsevier Ltd. All rights reserved.
doi:10.1016/j.carres.2009.05.026

Table 1
Comparison of the results obtained for *p*-nitrophenyl glycosides **1**–**6** using single-crystal and powder X-ray diffraction, as well as solid-state ^{13}C NMR

	Compound	Signals in ^{13}C CP MAS NMR	The number of molecules in the crystal asymmetric unit (XRD)	PXRD
1	*p*-Nitrophenyl α-D-galactopyranoside	Split	Two	One polymorph
2	*p*-Nitrophenyl β-D-galactopyranoside	Singlets	One	Two polymorphs (the unknown one in small amounts)
3	*p*-Nitrophenyl α-D-glucopyranoside	Split	Two[30,31]	One polymorph
4	*p*-Nitrophenyl β-D-glucopyranoside	Split	—	—
5	*p*-Nitrophenyl α-D-mannopyranoside	Split	Two (hemihydrate)[32] one (ethanol solvate)[33]	One polymorph (according to[32])
6	*p*-Nitrophenyl β-D-mannopyranoside	Split	—	—

appearing especially as polymorphs and solvates. Polymorphs may yield observably different NMR spectra, and, in suitable cases, valuable information can be obtained from chemical shifts of multiplets. In particular, the solid-state ^{13}C NMR data were helpful in the structural analysis of methyl glycopyranosides[28] and therefore it seemed interesting to characterize the anomeric pairs of *p*-nitrophenyl glycosides using NMR technique in conjunction with the X-ray diffraction analyses.

This paper is a continuation of our previous investigations focused on the structural properties of nitrophenyl glycosides. In our previous paper,[29] we have described the structure of six glycosides, the derivatives of D-glucose and D-galactose, focusing on per-*O*-acetyl derivatives of these glycosides. The current paper deals with the selected *p*-nitrophenyl glycosides with free hydroxyl groups, which, contrary to per-*O*-acetyl derivatives, can be used directly in the enzyme studies. We have chosen the derivatives of the monosaccharides, such as D-galactose, D-glucose, and D-mannose, which are most popular and widespread in nature.

2. Results and discussion

2.1. Single-crystal X-ray diffraction

For X-ray investigations the crystals of *p*-nitrophenyl α-D-galactopyranoside (**1**) and *p*-nitrophenyl β-D-galactopyranoside (**2**) were obtained by slow evaporation from ethanol/water solutions. The experimental data and structure refinement parameters are given in Table 2. Molecular structures and atom numbering are shown in Figures 1 and 2, whereas selected bond lengths, bond angles, and torsion angles are given in Table 3. The absolute configuration of **1** was assigned following the information obtained from Koch Light Laboratories Ltd, whereas that of **2** by the reference to the unchanging chiral centers of the precursor in the synthetic procedure.

Both **1** and **2** crystallize in $P2_1$ space group. An independent part of the unit cell is formed by two molecules of sugar in **1** (**1A** and **1B**) and by one molecule in **2**. Moreover, both **1** and **2** crystallize with one water molecule, which interacts with the sugar molecules by medium–strong hydrogen bonds. The packing in the crystals is determined by rather complex intermolecular networks of hydrogen bonds, involving all oxygen atoms of the hydroxyl groups, water molecules, nitro group, as well as a large number of intermolecular van der Waals interactions such as C–H···O and N···O. The selected interactions in the crystal lattice of **1** and **2** are shown in Figures 3 and 4, respectively. The strongest hydrogen bonds in **1** are formed between the water molecule and hydroxyl groups at C-6 (**1B**) and C-2 (**1A**) in which the water molecule plays a role of H-bond acceptor or donor, respectively. The O···O distances are 2.696 (2) Å in the former case and 2.776 (3) Å in the latter one. Another, much weaker hydrogen bond is formed between the water molecule and the nitro group of **1A** (the O···O distance is 3.068(2) Å). Several hydrogen bonds of comparable strength are also observed, which are formed between the hydroxyl groups at the pyranosidic ring of neighboring molecules, where they are either hydrogen bond donors or acceptors. In **2**, similarly to **1**, the strongest hydrogen bonds are also formed by the water molecule. Two of them involve the hydroxyl groups at C-3 of two neighboring molecules. One of the hydroxyl groups plays a role of hydrogen bond donor, another one of the acceptor (the O···O distances are 2.683 (2) Å and 2.735 (2) Å, respectively). The subsequent hydrogen bond involves the hydroxyl group at C-6, which plays a role of hydrogen bond acceptor (the O···O distance is 2.838 (2) Å). The hydrogen bonds formed by the hydroxyl groups at the pyranosidic ring are of similar strength in **2** as in **1** (their

Table 2
Crystal data and structure refinement for *p*-nitrophenyl α-D-galactopyranoside (**1**) and *p*-nitrophenyl β-D-galactopyranoside (**2**)

Compound	**1**	**2**
Molecular formula	$2C_{12}H_{15}NO_8{\cdot}H_2O$	$C_{12}H_{15}NO_8{\cdot}H_2O$
Molecular weight	620.52	319.27
Crystal system	Monoclinic	Monoclinic
Space group	$P2_1$	$P2_1$
Z (molecules/cell)	4	2
D_{calcd} Mg/m^3	1.555	1.554
Unit cell dimensions		
a (Å)	7.295 (2)	10.898 (2)
b (Å)	11.280 (2)	4.635 (1)
c (Å)	16.110 (3)	13.513 (3)
β (°)	90.88 (3)	91.13 (3)
Volume (Å^3)	1325 (5)	682.4 (2)
F(0 0 0) (e)	652	336
Wavelength (Å)	0.71073	0.71073
Absorption coefficient (mm^{-1})	0.134	0.135
Crystal size (mm^3)	0.3 × 0.2 × 0.15	0.4 × 0.2 × 0.15
Θ range for data collection (°)	3.57–25.00	3.74–24.99
Limiting indices	$-6 \leqslant h \leqslant 8$ $-3 \leqslant k \leqslant 13$ $-19 \leqslant l \leqslant 19$	$-12 \leqslant h \leqslant 12$ $-4 \leqslant k \leqslant 5$ $-16 \leqslant l \leqslant 16$
Reflections collected	9757	5053
Independent reflections	4584 [R_{int} = 0.0259]	1827 [R_{int} = 0.0342]
Data/restraints/parameters	4584/1/433	1827/1/224
Goodness-of-fit on F^2	0.993	1.062
Final R indices [$I > 2\sigma(I)$]	R_1 = 0.0277; wR_2 = 0.0630	R_1 = 0.0284; wR_2 = 0.0655
R indices (all data)	R_1 = 0.0320; wR_2 = 0.0651	R_1 = 0.0310; wR_2 = 0.0668
Extinction coefficient	0.024(2)	0.019(4)
Largest differences peak and hole $\Delta\rho$ (e/Å^3)	0.130 and −0.155	0.146 and −0.161

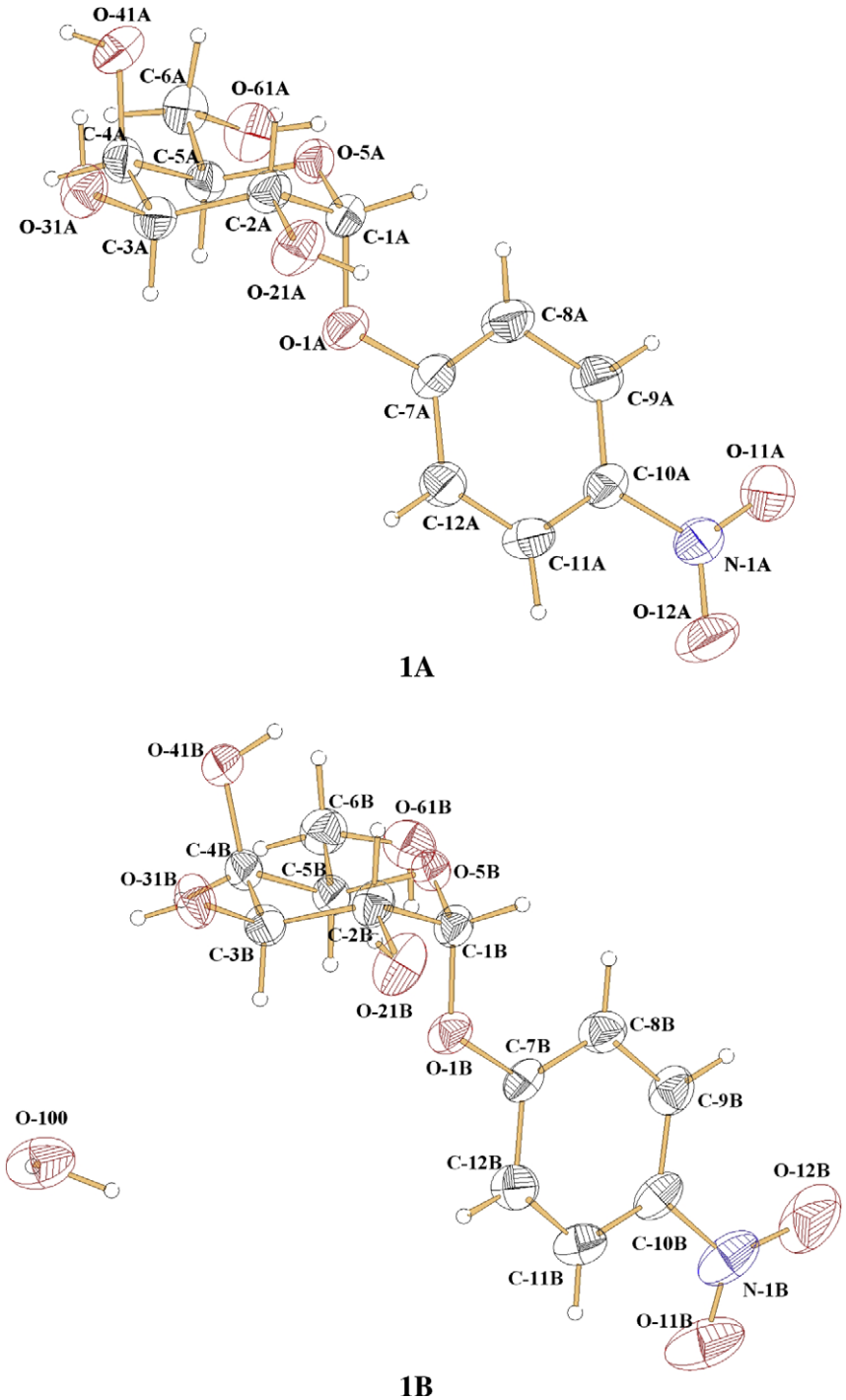

Figure 1. Molecular structure and atomic numbering of *p*-nitrophenyl α-D-galactopyranoside (**1A** and **1B**); the thermal ellipsoids are drawn at 50% probability.

O···O distances range between 2.735 (2) Å and 3.065 (2) Å) and involve the following interactions: O-41–H···O-31, O-21–H···O-21 and O-61–H···O-11. In both cases, **1** and **2**, a considerable number of weaker interactions, for example, C–H···O are also observed; the shortest ones being around 3.2 Å.

Similarly to **1** and **2**, both *p*-nitrophenyl α-D-glucopyranoside (**3**)[30,31] and *p*-nitrophenyl α-D-mannopyranoside (**5**)[32,33] crystallize in $P2_1$ space group. Two molecules also form an independent part of **3**[30,31] and hemihydrate of **5**,[32] whereas ethanol solvate of **5**[33] has one molecule in an independent part. Both **3**[30,31] and **5**[32,33] have essentially the same fragments participating in the hydrogen bond formation. Consequently, the strength of the hydrogen bonds is comparable to that of **1** and **2**. In **3** the O···O distances range between 2.740[30,31] and 3.109 Å[30] whereas in **5** they are between 2.737 (6)[32] and 3.128 (4) Å.[33]

The difference between **1** and **2** can be clearly observed in the geometry of the anomeric carbon atom (C-1). The C-1–O-5 and C-1–O-1 bond lengths and O-1–C-1–O-5 bond angles are clearly distinct. For **1** they range between 1.394 (2) Å and 1.400 (2) Å, 1.421(2) Å and 1.426(2) Å, and 113.6° (2) and 112.5° (1), respectively, while for **2** they are equal to 1.415 (2) Å, 1.404 (2) Å, and 106.5° (2), respectively. Such characteristic shortening of

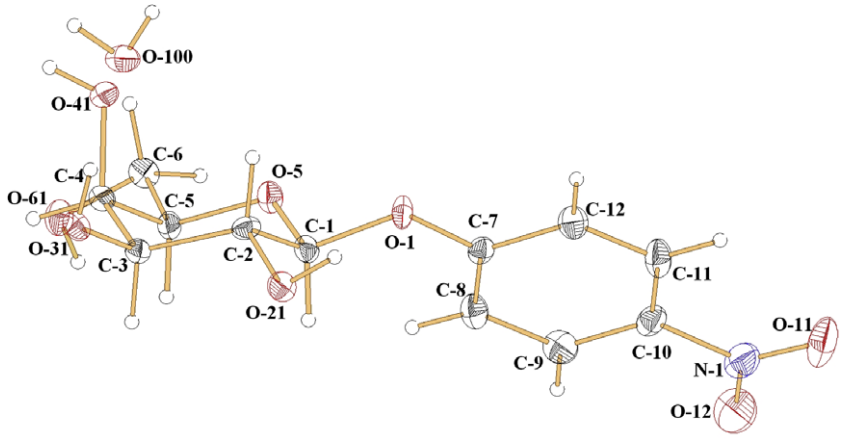

2

Figure 2. Molecular structure and atomic numbering of *p*-nitrophenyl β-D-galactopyranoside (**2**); the thermal ellipsoids are drawn at 50% probability.

Table 3
Selected bond lengths, bond angles, and major torsion angles for *p*-nitrophenyl α-D-galactopyranoside (**1**) and *p*-nitrophenyl β-D-galactopyranoside (**2**)

Atoms	Compound		
	1A	**1B**	**2**
Bond lengths (Å)			
C-1–O-5	1.394 (2)	1.400 (2)	1.415 (2)
C-1–O-1	1.421 (2)	1.426 (2)	1.404 (2)
C-5–O-5	1.444 (2)	1.446 (2)	1.442 (2)
O-1–C-7	1.367 (2)	1.360 (2)	1.367 (2)
Bond angles (°)			
O-1–C-1–O-5	113.6 (2)	112.5 (1)	106.5 (2)
C-1–O-5–C-5	115.2 (1)	113.9 (1)	111.4 (1)
C-1–O-1–C-7	119.2 (1)	120.7 (1)	119.3 (2)
Torsion angles (°)			
O-1–C-1–O-5–C-5	63.3 (2)	57.3 (2)	−177.1 (1)
O-5–C-1–O-1–C-7	83.0 (2)	69.3 (2)	−84.1 (2)
C-2–C-1–O-1–C-7	−154.6 (2)	−169.4 (2)	156.2 (2)
C-1–O-1–C-7–C-8	−18.2 (3)	−4.0 (3)	12.1 (3)
C-1–O-1–C-7–C-12	161.9 (2)	175.6(2)	−168.2 (2)
C-11–C-10–N-1–O-11	179.5 (2)	14.0 (3)	4.2 (3)
C-9–C-10–N-1–O-12	178.6 (2)	14.6 (3)	5.8 (3)
O-1–C-7–C-12–C-11	−177.7 (2)	178.3 (2)	177.5 (2)

C-1–O-5 bond and lengthening of C-1–O-1 bond in **1** (α anomer) in comparison to **2** (β anomer) are undoubtedly connected with the anomeric effect. The comparison of geometries of **3**[30,31] and **5**,[32,33] leads to the conclusion that the largest structural changes are observed for the fragments whose configurations differ from each other. It obviously concerns the C-4 carbon atom in **1** and the C-2 and C-4 fragments in **2**.

Interestingly, neither in **1**, nor in **2**, the nitro group is coplanar with the phenyl ring. The angles between the best planes estimated for these fragments are 2.4°, 14.8°, and 5.1° for **1A**, **1B**, and **2**, respectively. This effect has been observed and quantified in acetylated gluco- and galactopyranosides[29] and supports the view[34] that the nitro group does not effectively conjugate with the benzene ring and even weak interactions in the solid-state may easily twist it. This effect is also observed in **3**, where the twist angle is equal to 12.8° or 16.3° (for two independent molecules)[30,31] and in **5**, where the angle may range from 2.0°[33] to 8.2°.[32]

The sugar moieties of **1** and **2** adopt $^4C_1$ conformation. The Cremer–Pople puckering parameter[35] Θ for **2** is equal to 4.2 (2)°, while the other puckering parameters, Q and φ, are equal to 0.579 (2) and 310 (3)°, respectively. For **1**, Θ, Q, and φ are equal to 3.1 (2)°, 0.543 (2) and 143 (3)° and 2.0 (2)°, 0.556 (2) and 23 (5)°, respectively, for molecules A and B. For other related systems, Θ, Q and φ are equal to 7.4° or 3.6°[30] (6.2° or 4.8°),[31] 0.561 or 0.542[30] (0.562 or 0.538),[31] 303.85° or 55.10°[30] (309.19° or 58.04°)[31] for two independent molecules of **3** and are equal to 5.2° (6) or 5.3° (6)[32] (4.9° (5)),[33] 0.561 (6) or 0.557 (6)[32] (0.528 (4)),[33] 80° (6) or 265° (7)[32] (76° (6))[33] for **5**.

2.2. ^{13}C CP MAS NMR spectroscopy

The ^{1}H and ^{13}C NMR spectra were recorded for **1**–**6** in DMSO-d_6 solutions. The 2D experiments were helpful to achieve a complete assignment of the proton and carbon chemical shifts (Table 4). The ^{13}C CP MAS NMR spectra were recorded for solid compounds at 10 kHz with RAMP shape CP sequence. The resonances in the solid-state spectra were assigned following the same sequence as in the solution spectra. The spectra of both **1** and **2**, as well as those of **3** and the ethanol solvate of **4**, are shown in Figures 5 and 6, respectively. The resonances of aromatic carbon atoms could be easily distinguished from those of C–H carbon atoms of sugars. The chemical shifts for solid *p*-nitrophenyl glycopyranosides **1**–**6** are collected in Table 4, together with the differences $\Delta = \delta_{solution} - \delta_{solid}$.

Besides the intramolecular (steric) effects, intermolecular interactions should also be taken into account while analyzing the NMR spectra. In the solids, as well as in DMSO-d_6 solutions, the sugar hydroxyl groups are involved in O–H···O hydrogen bonds. Therefore, chemical shifts for C–OH carbon atoms are close in both phases; larger differences amounting to 2–3.5 ppm observed for C-5 and C-6, probably result from conformational differences (frozen rotation of CH_2OH moiety). The packing in the crystal is determined by the intermolecular network of hydrogen bonds and a number of van der Waals interactions. Water or ethanol molecules act as additional hydrogen bond donors (**4**, **5**). In the spectrum of **4** one can observe the ^{13}C resonances of the ethanol at 59.4 and 15.2 ppm (Fig. 6b); complex pattern of hydrogen bond interactions involving the disordered ethanol molecules is reflected in the multiplicity of sugar resonances.

In the solid-state spectra of **1** and **3**–**6** the number of resonances exceeded the number of carbon atoms in the molecule, suggesting that there are at least two different molecules in the independent unit cell. The doublets of C-1 and C-7, as well as of C-10, can be easily recognized (Fig. 5a). The main differences between these molecules are the relative orientations of the pyranosidic and aromatic rings, as indicated by the XRD data for **1**, **3**, and **5** (there is no X-ray structure for **6**). However, the structural differences may also result from two orientations of the aromatic ring, the resonances of C-1

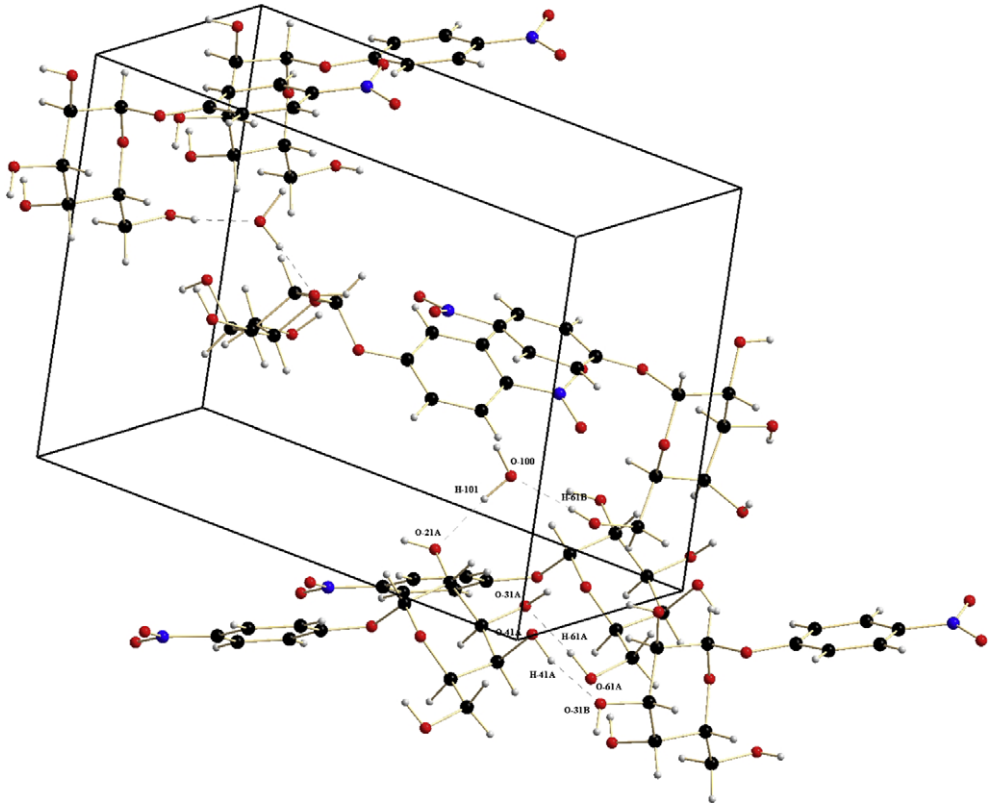

Figure 3. Crystal packing of *p*-nitrophenyl α-D-galactopyranoside (**1**); hydrogen bonds are indicated as dashed lines.

and C-7 appeared as singlets, whereas the resonances of C-8 and C-12 are split.

In the solid-state spectrum of **2**, distinct singlet resonances are observed, suggesting that **2** consists of only one kind of magnetically equal molecules. Therefore it seems, at this stage of investigations, that **2** exists as one polymorphic form which probably corresponds to the data obtained from single-crystal X-ray diffraction. However, in the next section, some new details will be discussed according to the structure of **2**.

In solutions, the *p*-nitrophenyl group (aglycon) can rotate freely, in solids the equilibration is usually inhibited revealing specific environments with different chemical shifts. Separate signals of both C-8 and C-12, as well as of both C-9 and C-11, (the carbon atoms in the aromatic ring) were visible in the solid-state spectra. The splitting (of 3.1–10.5 ppm) is clearly observable especially for C-8 and C-12. One can expect that the chemical shifts of C-7, C-8 and C-12 reflect the conjugation of free electron pairs of glycosidic oxygen atom with the aromatic system (as suggested by the length of the C-7–O-1 bond which is shorter than the typical single one), and that they are sensitive to the twist angle of the aromatic ring. However, there is no simple relationship between the length of C-7–O-1 bond and chemical shift of C-7. Larger dihedral angle between the aromatic ring and the plane of C-1, C-7, and O-1 (glycosidic oxygen atom) results in a relatively close approach between the atoms of the sugar residues and C-8 and C-12 of the aromatic ring (and can be relieved by the enlargement of the valence angles).

2.3. Powder X-ray diffraction

The confirmation of the crystal structures and NMR data for **1**–**3** and **5** was obtained from the powder X-ray diffraction patterns (Table 1). The experimental powder X-ray diffraction patterns of **1** (Fig. 7), **3** (Fig. 8) and **5** (Fig. 9) closely match those calculated from a single-crystal X-ray diffraction refinement in 2θ angles. The observed small variation in the relative peak intensities is subjected to the preferred orientation effects. This confirms the presence of the particular crystal forms in the samples. Therefore, the splitting of resonances in ^{13}C CP MAS NMR spectrum of **1**, **3**, and **5** seems to be caused by two non-equivalent molecules in the independent part of the crystal unit, and not by two polymorphs existing in these samples (Table 1).

Powder X-ray diffraction pattern for **2** (Fig. 10) indicated the presence of two polymorphs, monohydrate of *p*-nitrophenyl β-D-galactopyranoside (monoclinic system with space group $P2_1$ and cell parameters: $a = 10.898(2)$ Å, $b = 4.6350(9)$ Å, $c = 13.513(3)$ Å, $\beta = 91.13(3)^\circ$, and $V = 682.44$ Å^3) and another unknown crystal form present in a small amount. Due to such a small content of this unknown polymorphic form it was impossible to determine the parameters of its unit cell. The unit cell parameters of the monoclinic form were refined from its diffraction patterns using a full-pattern profile fitting method using the program GSAS[36] (Fig. 11). The parameters of the refined unit cell are $a = 10.924(1)$ Å, $b = 4.6689(5)$ Å, $c = 13.705(1)$ Å, $\beta = 91.76(1)^\circ$, and $V = 698.70$ Å^3. The resulting volume of the unit cell is slightly larger. This may be the result of the greater water content in monoclinic form of *p*-nitrophenyl β-D-galactopyranoside in **2**.

3. Experimental

3.1. *p*-Nitrophenyl α-D-galactopyranoside (1)

This compound was purchased from Koch Light Laboratories Ltd.

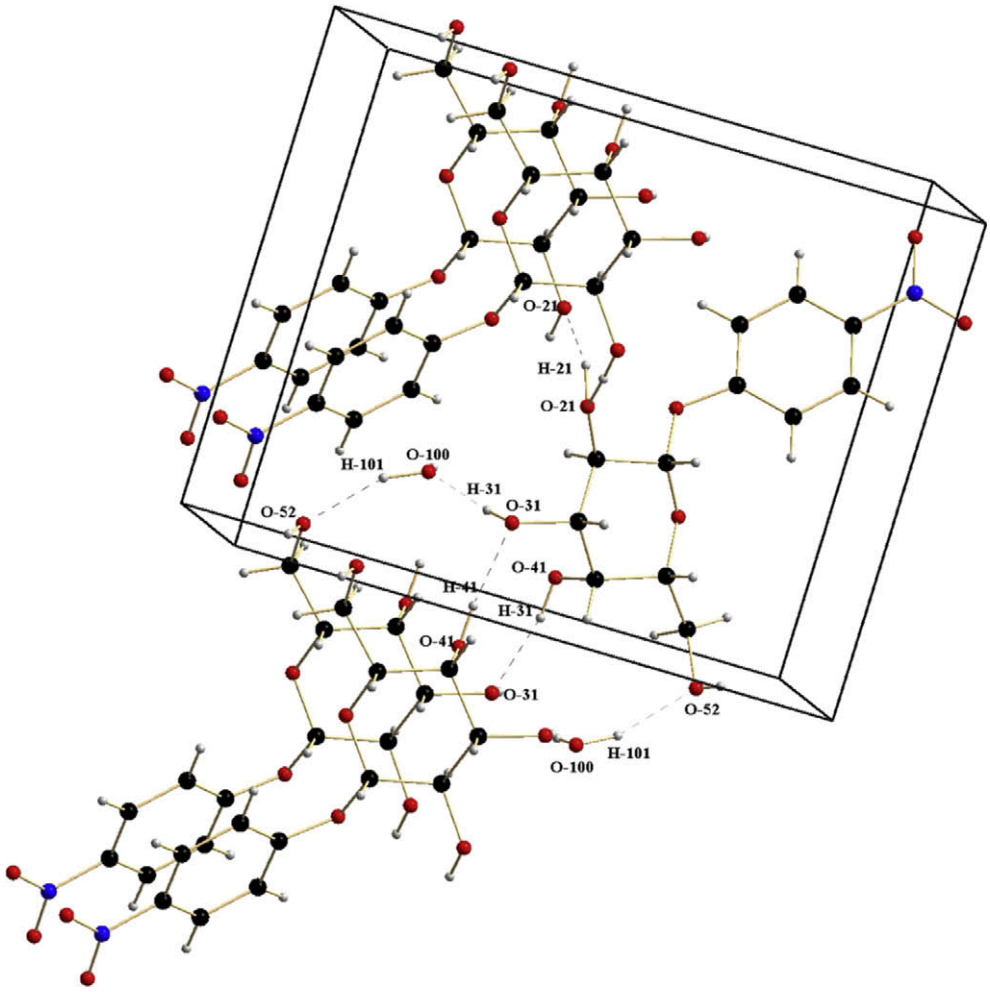

Figure 4. Crystal packing of *p*-nitrophenyl β-D-galactopyranoside (**2**); hydrogen bonds are indicated as dashed lines.

Table 4
The ^{13}C NMR chemical shifts (δ, ppm) for *p*-nitrophenyl glycopyranosides **1**–**6** in: DMSO-d_6 solutions ($\delta_{solution}$); solid phase (δ_{solid}) and the differences $\Delta = \delta_{solution} - \delta_{solid}$ >1 ppm (given in parentheses)

Atom	Compound											
	1		**2**		**3**		**4**		**5**		**6**	
	δ_{solid}	$\delta_{solution}$	δ_{solid}	$\delta_{solution}$	δ_{solid}	$\delta_{solution}$	δ_{solid}	$\delta_{solution}$	δ_{solid}	$\delta_{solution}$	δ_{solid}	$\delta_{solution}$
C-1	98.7/96.7 (−/−1.4)	98.05	100.4	101.29	98.8/97.7 (−1.2/−)	97.65	100.1/98.7	99.69	96.2 (2.4)	98.58	97.7	97.23
C-2	68.3	67.64	70.3	70.95	69.9 (1.3)	71.19	73.2/70.9 (−/2.1)	72.95	70.1	69.59	70.4/72.0 (−/−2.0)	69.98
C-3	72.4 (−3.2)	69.25	74.8	73.97	72.1	72.83	79.1/76.2 (−2.0/−)	77.08	71.5 (−1.1)	70.42	74.4 (−1.3)	73.09
C-4	70.7 (−2.4)	68.35	70.3	68.91	68.1 (1.5)	69.59	67.2/65.8 (2.1/3.5)	69.34	66.0/64.9 (−/1.5)	66.41	65.5/63.7 (−/2.8)	66.50
C-5	75.0 (−2.1)	72.86	77.5	76.56	75.1	74.26	74.5/73.2 (1.8/3.1)	76.29	73.3 (2.1)	75.43	77.9	77.73
C-6	63.9 (−3.8)	60.15	61.3	61.16	59.1 (1.4)	60.49	62.5/61.8 (−2.1/−1.4)	60.38	60.3	60.82	60.9/59.9	60.79
C-7	165.1/162.6 (−2.7/−)	162.43	161.4	163.32	161.2	162.16	160.7 (1.6)	162.28	160.1/158.8 (1.2/2.5)	161.34	162.8	162.05
C-8	121.3/116.5 (−4.5/−)	116.85	113.9	117.35	121.7/113.7 (−4.9/3.1)	116.81	117.2/113.6 (−/2.8)	116.42	120.1 (−3.3)	116.76	119.1/117.6 (−2.8/−1.3)	116.31
C-9	127.5/125.3 (−1.9/−)	125.61	124.8	126.55	125.0	125.63	126.5/123.7 (−/1.9)	125.60	124.5 (1.1)	125.62	122.8/121.8 (2.8/3.8)	125.59
C-10	143.3/141.5 (−1.9/−)	141.41	140.2	142.40	141.5	141.47	142.2	141.53	143.1/141.5 (−1.6/−)	141.52	140.4/139.1 (−/2.3)	141.39
C-11	127.5/125.3 (−1.9/−)	125.61	127.0	126.55	125.0	125.63	126.5/123.7 (−/1.9)	125.60	124.5	125.62	125.3/124.0 (−/1.6)	125.59
C-12	118.8/115.7 (−2.0/1.2)	116.85	113.9	117.35	120.0/111.2 (−3.2/5.6)	116.81	115.6/112.4 (−/4.0)	116.42	115.1/113.5 (1.7/3.3)	116.76	114.5/113.9 (1.8/2.4)	116.31

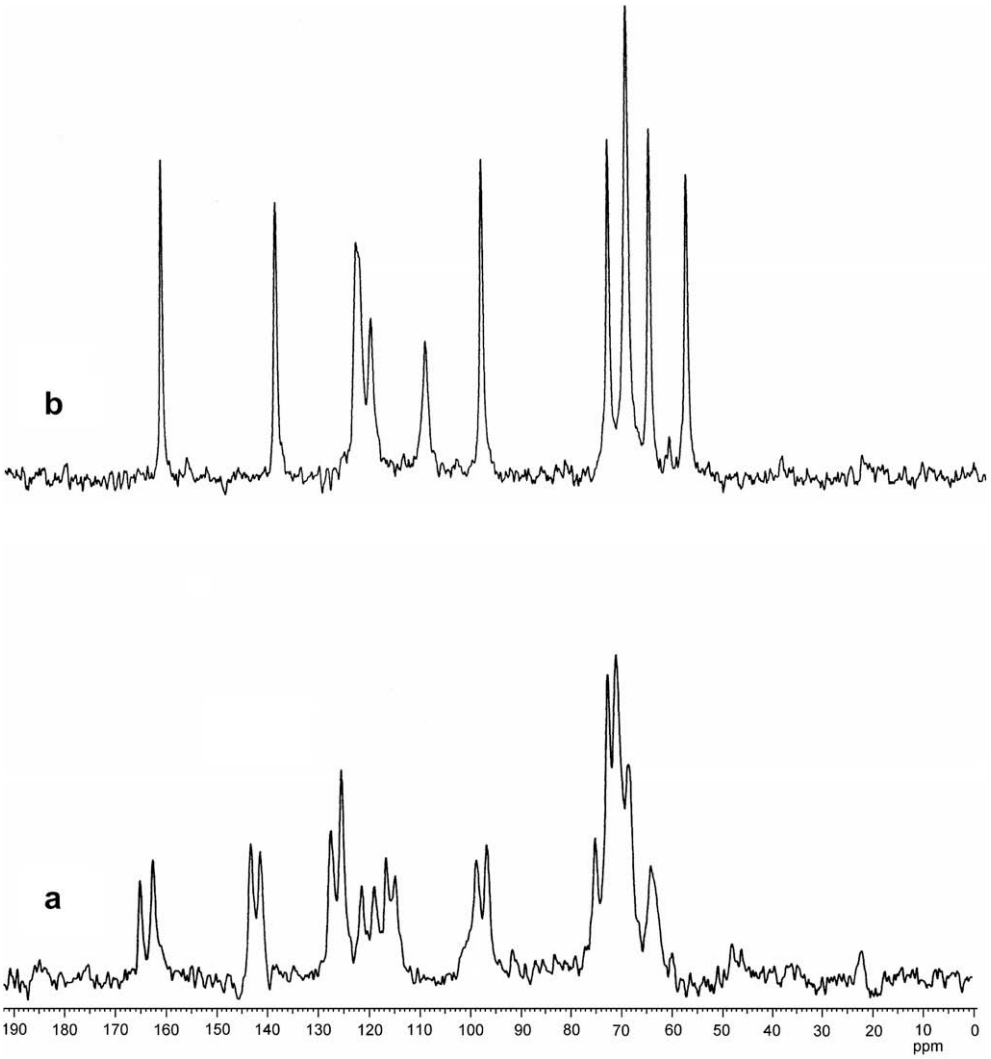

Figure 5. ^{13}C CP MAS NMR spectra of (a): *p*-nitrophenyl α-D-galactopyranoside (**1**) and (b): *p*-nitrophenyl β-D-galactopyranoside (**2**); rotation speed of 10 kHz.

3.2. *p*-Nitrophenyl β-D-galactopyranoside (2)

Deacetylation of *p*-nitrophenyl 2,3,4,6-tetra-*O*-acetyl-β-D-galactopyranoside[29] by Zemplén method gave **2** as white crystals; mp 180–182 °C, $[\alpha]_D^{20}$ −80.6 (*c* 0.5, H_2O); lit.[37] mp 180–182 °C, $[\alpha]_D^{23}$ −79.5 (*c* 1, H_2O).

3.3. *p*-Nitrophenyl α-D-glucopyranoside (3)

This compound was purchased from Sigma–Aldrich Chemie GmbH.

3.4. *p*-Nitrophenyl β-D-glucopyranoside (4)

This compound was obtained from *p*-nitrophenyl 2,3,4,6-tetra-*O*-acetyl-β-D-glucopyranoside[29] according to the procedure that was the same as that used for obtaining **2**. White crystals; mp 166–167 °C, $[\alpha]_D^{20}$ −102.3 (*c* 1, H_2O) lit.[38] mp 165–167 °C; lit.[39] $[\alpha]_D^{25}$ −108.3 (H_2O).

3.5. *p*-Nitrophenyl α-D-mannopyranoside (5) and *p*-Nitrophenyl β-D-mannopyranoside (6)

These compounds were purchased from Sigma–Aldrich Chemie GmbH.

3.6. Physical measurements

The ^1H and ^{13}C NMR spectra for DMSO-d_6 solutions were recorded on a Bruker DRX-400 spectrometer; the (2D) ^1H–^{13}C correlations were run using standard pulse programs from Bruker library. Solid-state ^{13}C cross-polarization (CP) magic angle spinning (MAS) spectra were recorded on a Bruker DRX-400 spectrometer at 100.61 MHz. Powder samples were spun at 10 kHz in a 4 mm ZrO_2 rotor (a contact time of 2 ms, a repetition time of 6 s, and 600 scans). ^{13}C chemical shifts were calibrated indirectly through the glycine CO signal recorded at 176.0 ppm, relative to TMS.

The X-ray diffraction measurements of **1** and **2** were performed on a KUMA CCD κ-axis diffractometer with graphite-monochromated Mo Kα radiation (0.71073 Å) at 150 ± 2 K and 100 ± 2 K, respectively. The crystals were positioned at 62.3 mm from the KM4CCD camera. 664 frames were measured at 0.9° intervals with a counting time of 20 s, and 664 frames were measured at 0.9° intervals with a counting time of 40 s, respectively. The data were corrected for Lorentz and polarization effects. The numerical absorption correction was not applied. Data reduction and analysis were carried out with the Kuma Diffraction (Wrocław, Poland) programs.[40] The structures were solved by direct methods[41] and refined using SHELXL.[42] The refinement was based on F^2 for all reflections except for those with very negative F^2. The weighted

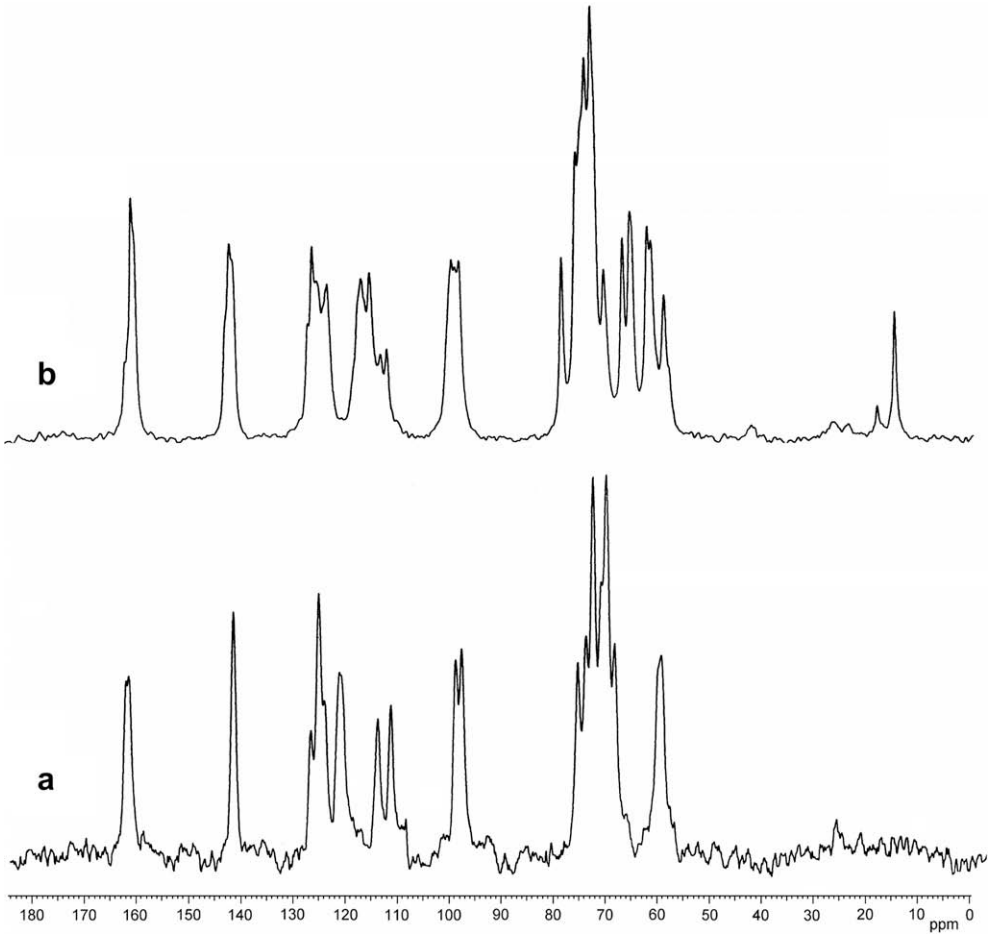

Figure 6. ^{13}C CP MAS NMR spectra of (a): *p*-nitrophenyl α-D-glucopyranoside (**3**) and (b): *p*-nitrophenyl β-D-glucopyranoside (**4**); rotation speed of 10 kHz.

R factor, *wR*, and all goodness-of-fit *S* values are based on F^2. The non-hydrogen atoms were refined anisotropically, whereas the H-atoms were placed in the calculated positions; their positions and thermal parameters were refined isotropically. Scattering factors were taken from Tables 6.1.1.4 and 4.2.4.2.[43] Crystal data together with the data collection and structure refinement details are listed out in Table 2.

The powder X-ray diffraction patterns of **1**–**3** and **5** were recorded on a Seifert HZG-4 automated diffractometer using Cu $K\alpha_{1,2}$ radiation (1.5418 Å). The data were collected in the Brag-

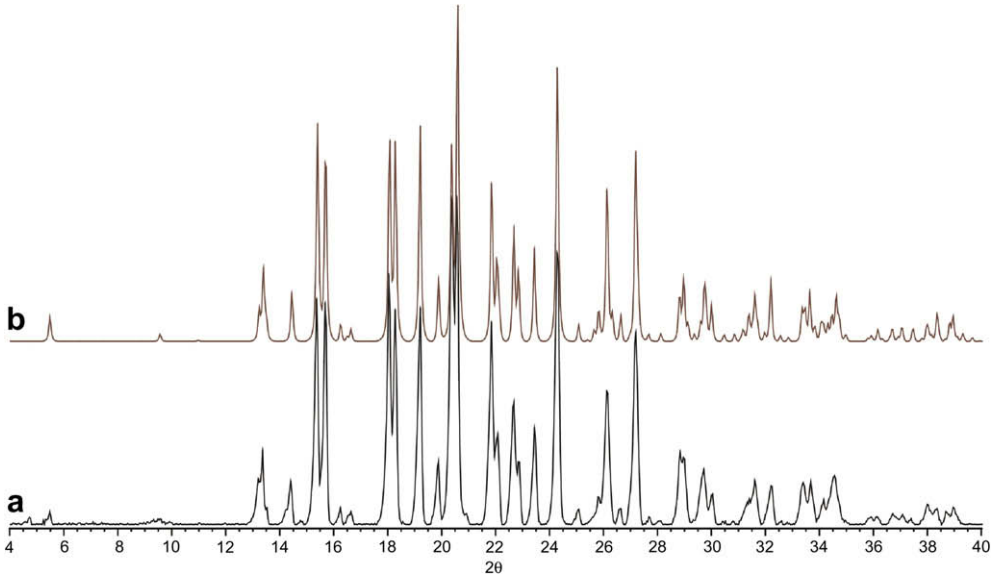

Figure 7. PXRD pattern of **1** (a) and theoretically calculated pattern of *p*-nitrophenyl α-D-galactopyranoside (b).

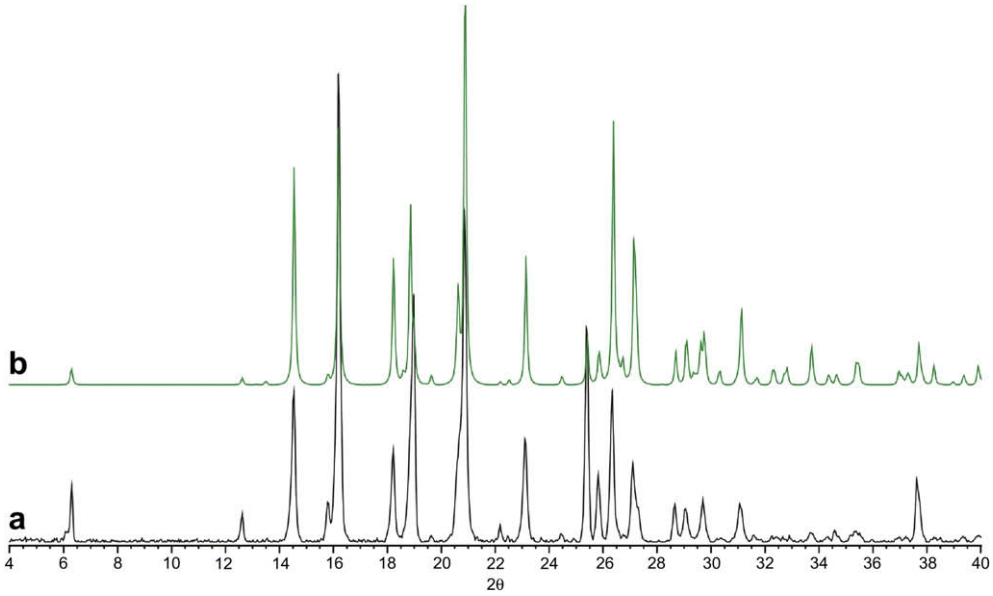

Figure 8. PXRD pattern of **3** (a) and theoretically calculated pattern of *p*-nitrophenyl α-D-glucopyranoside (b).[30]

Brentano ($\theta/2\theta$) horizontal geometry (flat reflection mode) between 4 and 40° (2θ) in 0.04° steps, at 5 s step^{-1}. The optic of the HZG-4 diffractometer was a system of primary Soller slits between the X-ray tube and the fixed aperture slit of 2.0 mm. One scattered-radiation slit of 2 mm was placed after the sample, followed by the detector slit of 0.2 mm. The X-ray tube operated at 40 kV and 40 mA. Powder XRD patterns were simulated from single-crystal data using the program MERCURY.[44]

4. Conclusions

The structural analyses of *p*-nitrophenyl glycopyranosides, the derivatives of D-galactose, D-glucose, and D-mannose, often used in enzymology as markers, were performed using the following experimental techniques: single-crystal X-ray diffraction (XRD) for **1** and **2**, ^{13}C NMR spectroscopy in both solid and solution phases for **1**–**6**, and the powder X-ray diffraction (PXRD) for **1**–**3** and **5** (Table 1). According to the XRD measurements, **1** and **2** crystallize with one water molecule which interacts with sugar molecules by hydrogen bonds. In **1** and **2** a complex hydrogen bond network is observed. There are two independent molecules in the crystal unit cell in **1**, whereas in **2** there is one molecule. The most distinct structural differences between both molecules of **1** (**1A** and **1B**) are found in the torsion angles around the hydroxyl groups at C-2, C-4, and C-6, while the most significant differences between structures of **1** and **2** are connected with the geometry at the anomeric carbon atom. Therefore, due to the anomeric effect, characteristic lengthening and shortening of appropriate bond lengths are observed between the two anomers. In both **1** and **2**, the nitro group is not coplanar with the benzene ring. Moreover, the molecules of **1** and **2** adopt slightly disordered $^4C_1$ conformations.

In solid-state NMR spectra, separate signals of C-8 and C-12 as well as of C-9 and C-11 are detected and this phenomenon

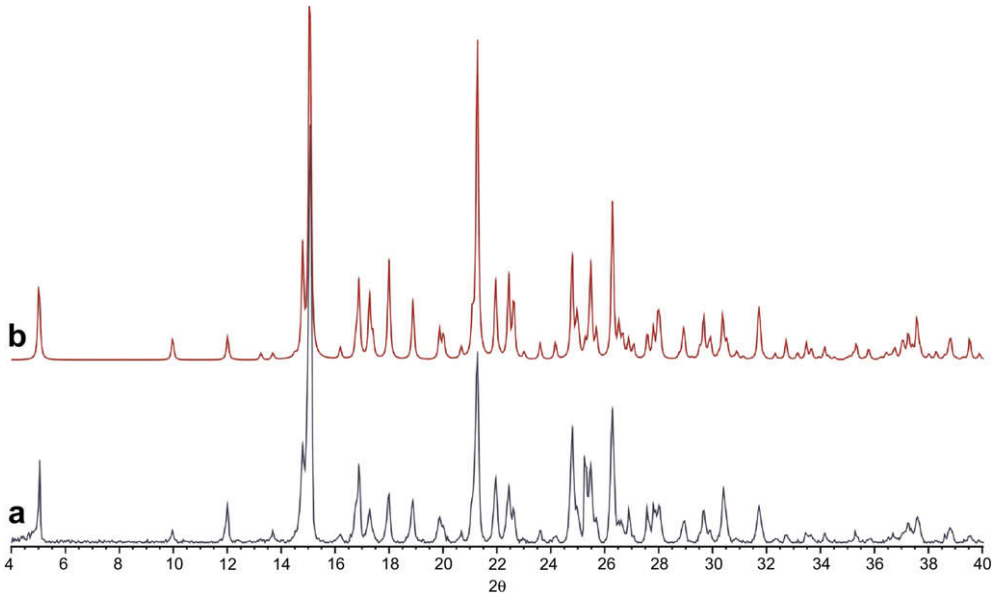

Figure 9. PXRD pattern of **5** (a) and theoretically calculated pattern of *p*-nitrophenyl α-D-mannopyranoside (b).[32]

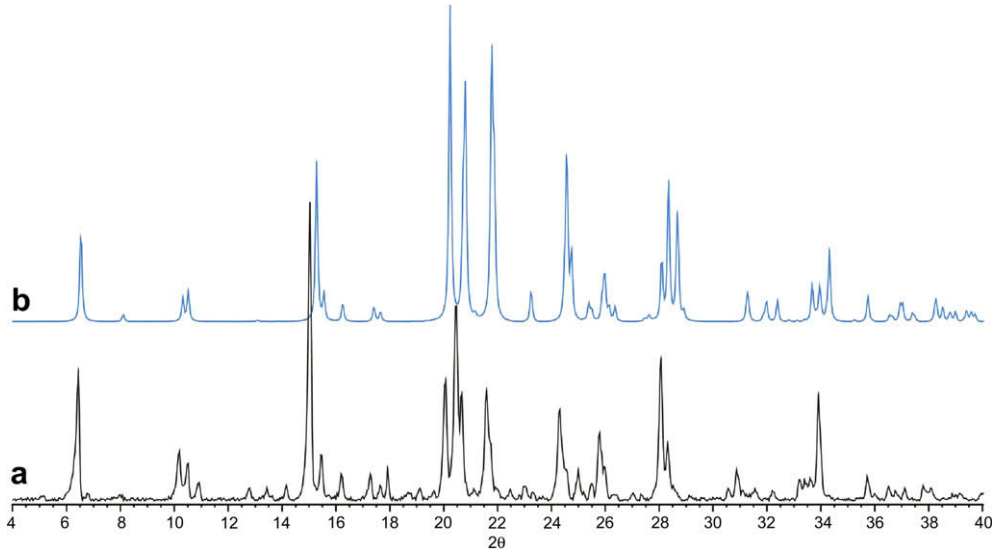

Figure 10. PXRD pattern of **2** (a) and theoretically calculated pattern of *p*-nitrophenyl β-D-galactopyranoside (b).

is connected with a frozen rotation of the *p*-nitrophenyl group, the aglycon, in the solid phase in contrast to the solution phase in which this group can rotate freely. In contrast, the resonances of carbon atoms bearing hydroxyl groups are similar in both solid and solution phases, because of the existence of hydrogen bonds in both cases. Solid **4** exists as ethanol solvate, as suggested by the characteristic signals in the solid-state ^{13}C NMR spectrum. For **1** and **3**–**6** two magnetically non-equivalent molecules are detected, while separate signals have been noticed for **2**.

The powder X-ray diffraction patterns reveal that **1**, **3**, and **5** consist of only one polymorphic phase which corresponds to the appropriate XRD measurements, so the splitting of resonances in the solid-state spectra of these compounds is caused not by two polymorphs, but by two magnetically different molecules in the separate polymorph. The PXRD pattern for **2** indicates the existence of two polymorphic forms, one of them is unknown, and the subsequent one is similar to the calculated pattern. The slight difference between the XRD and PXRD of **2** is connected with a bigger volume of the unit cell in the macroscopic sample

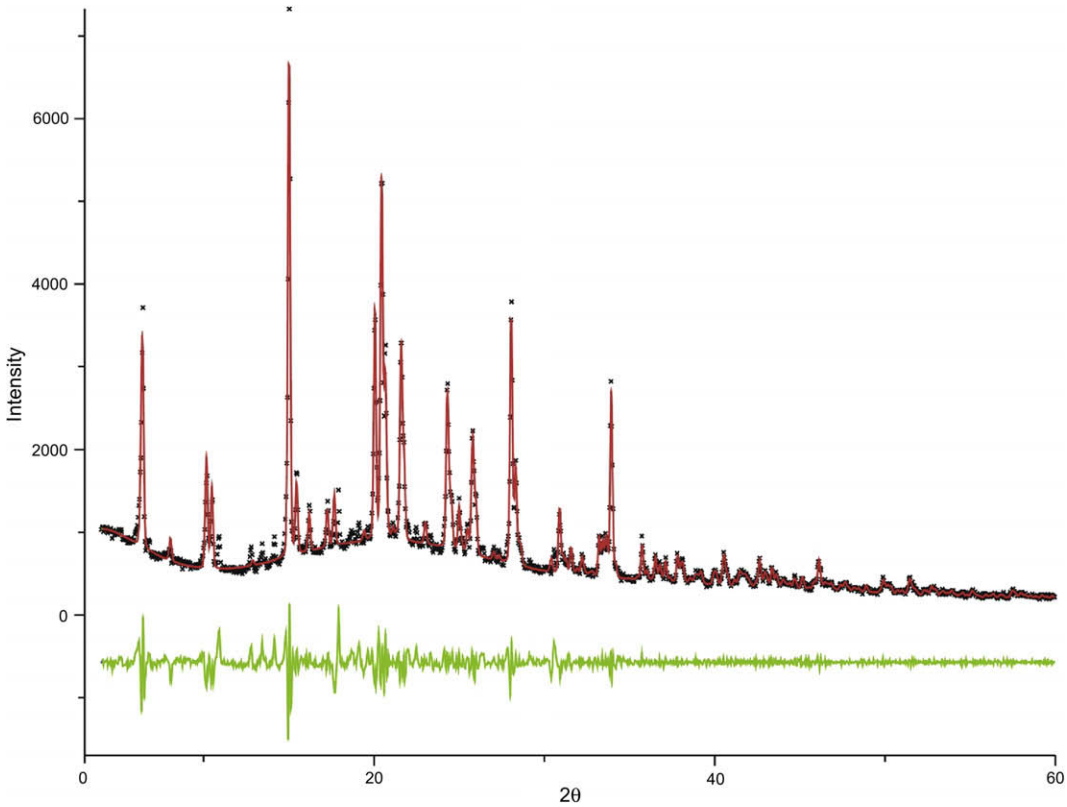

Figure 11. Experimental (×), calculated (red, solid line), and difference (green, lower line) PXRD profiles for the LeBail fitting of *p*-nitrophenyl β-D-galactopyranoside (**2**).

used in PXRD in contrast to the single-crystal sample employed in XRD. Furthermore, this difference could be connected with the greater water content in the polymorph of the macroscopic sample.

5. Supplementary data

Crystallographic data for the structures have been deposited with the Cambridge Crystallographic Data Centre as supplementary publication no. CCDC 721648 (**1**) and CCDC 721649 (**2**). Copies of the data can be obtained on application to CCDC, 12 Union Road, Cambridge CB2 1EZ, UK (email: deposit@ccdc.cam.ac.uk).

Acknowledgments

Financial support from the University of Warsaw (BST-132 652) and the Medical University of Warsaw (FW-28/N/2008) is gratefully acknowledged. The X-ray measurements were performed in the Crystallographic Unit of the Physical Chemistry Laboratory at the Faculty of Chemistry of the University of Warsaw.

References

1. Collins, P.; Ferrier, R. In *Monosaccharides: Their Chemistry and Their Roles in Natural Products*; John Wiley & Sons: Chichester, 1995; pp 506–510.
2. Legler, G. *Adv. Carbohydr. Chem. Biochem.* **1990**, *48*, 319–385.
3. Legler, G. In *Iminosugars as Glycosidase Inhibitors*; Stütz, A. E., Ed.; Wiley-VCH: Weinheim, 1999; pp 31–36.
4. Sinnott, M. L. *Chem. Rev.* **1990**, *90*, 1171–1202.
5. Davies, G.; Sinnott, M. L.; Withers, S. G. In *Comprehensive Biological Catalysis*; Sinnott, M. L., Ed.; Academic Press: New York, 1998; pp 119–208.
6. Namchuk, M. N.; Withers, S. G. *Biochemistry* **1995**, *34*, 16194–16202.
7. Mosi, R.; Sham, H.; Uitdehaag, J. C. M.; Ruiterkamp, R.; Dijkstra, B. W.; Withers, S. G. *Biochemistry* **1998**, *37*, 17192–17198.
8. Withers, S. G.; Namchuk, M.; Mosi, R. In *Iminosugars as Glycosidase Inhibitors*; Stütz, A. E., Ed.; Wiley-VCH: Weinheim, 1999; pp 188–206.
9. Ly, H.; Withers, S. G. *Annu. Rev. Biochem.* **1999**, *68*, 487–522.
10. Zechel, D. L.; Withers, S. G. *Acc. Chem. Res.* **2000**, *33*, 11–18.
11. Rye, C. S.; Withers, S. G. *Curr. Opin. Chem. Biol.* **2000**, *4*, 573–580.
12. Davies, G.; Henrissat, B. *Structure* **1995**, *3*, 853–859.
13. White, A.; Rose, D. R. *Curr. Opin. Struct. Biol.* **1997**, *7*, 645–651.
14. Wolfenden, R.; Lu, X.; Young, G. *J. Am. Chem. Soc.* **1998**, *120*, 6814–6815.
15. Heightmann, T. D.; Vasella, A. T. *Angew. Chem., Int. Ed.* **1999**, *38*, 750–770.
16. Vasella, A.; Davies, G. J.; Böhm, M. *Curr. Opin. Chem. Biol.* **2002**, *6*, 619–629.
17. Pazur, J. H. *Adv. Carbohydr. Chem. Biochem.* **1981**, *39*, 405–447.
18. Voorhees, V.; Adams, R. *J. Am. Chem. Soc.* **1922**, *44*, 1397–1405.
19. Neilson, T.; Wood, H. C. S.; Wylie, A. G. *J. Chem. Soc.* **1962**, 371–372.
20. Bloch, R.; Burger, M. M. *FEBS Lett.* **1974**, *44*, 286–289.
21. Duerksen, J. D.; Halvorson, H. *J. Biol. Chem.* **1958**, *233*, 1113–1120.
22. Legler, G. *Hoppe-Seyler's Z. Physiol. Chem.* **1967**, *348*, 1359–1366.
23. Hösel, W.; Nahrstedt, A. *Hoppe-Seyler's Z. Physiol. Chem.* **1975**, *356*, 1265–1275.
24. Weber, J. P.; Fink, A. L. *J. Biol. Chem.* **1980**, *255*, 9030–9032.
25. Ohnishi, M.; Okada, G.; Yazaki, T. *Carbohydr. Res.* **1998**, *308*, 201–205.
26. Hansson, T.; Andersson, M.; Wehtje, E.; Adlercreutz, P. *Enzyme Microb. Technol.* **2001**, *29*, 527–534.
27. Harris, R. K. *Analyst* **2006**, *131*, 351–373.
28. Paradowska, K.; Gubica, T.; Temeriusz, A.; Cyrański, M. K.; Wawer, I. *Carbohydr. Res.* **2008**, *343*, 2299–2307.
29. Temeriusz, A.; Gubica, T.; Rogowska, P.; Paradowska, K.; Cyrański, M. K. *Carbohydr. Res.* **2005**, *340*, 1175–1184.
30. Swaminathan, P. *Acta Crystallogr., Sect. B* **1982**, *38*, 184–188.
31. Jones, P. G.; Sheldrick, G. M. *Z. Kristallogr.* **1982**, *161*, 69–77.
32. Fernandez-Castaño, C.; Foces-Foces, C. *Acta Crystallogr., Sect. C* **1996**, *52*, 1586–1588.
33. Agianian, B.; Perrakis, A.; Kanellopoulos, P. N.; Sheldrick, B.; Hamodrakas, S. J. *Acta Crystallogr., Sect. C* **1997**, *53*, 811–814.
34. (a) Boese, R.; Blaser, D.; Nussbaumer, M.; Krygowski, T. M. *Struct. Chem.* **1992**, *3*, 363–368; (b) Exner, O.; Krygowski, T. M. *Chem. Soc. Rev.* **1996**, *25*, 71–75; (c) Dobrowolski, M. A.; Krygowski, T. M.; Cyrański, M. K. *Croat. Chem. Acta*, in press.
35. (a) Cremer, D.; Pople, J. A. *J. Am. Chem. Soc.* **1975**, *97*, 1354–1358; (b) Cremer, D. *Acta Crystallogr., Sect. B* **1984**, *40*, 498–500.
36. Larson, A. C.; Von Dreele, R. B. GSAS; Los Alamos Laboratory Report No. LA-UR-86-748, 1987.
37. Matta, K. L.; Barlow, J. J. *Carbohydr. Res.* **1977**, *53*, 209–216.
38. Liu, H.-M.; Yan, X.; Li, W.; Huang, C. *Carbohydr. Res.* **2002**, *337*, 1763–1767.
39. Arita, H.; Sugita, K.; Nomura, A.; Sato, K.; Kawanami, J. *Carbohydr. Res.* **1978**, *62*, 143–154.
40. Oxford Diffraction *CrysAlis CCD and CrysAlis RED*; Oxford Diffraction Poland: Wrocław, Poland, 2001.
41. Sheldrick, G. M. *Acta Crystallogr., Sect. A* **1990**, *46*, 467–473.
42. Sheldrick, G. M. SHELXL*93. Program for the Refinement of Crystal Structure*; Germany: University of Göttingen, 1993.
43. *International Tables for Crystallography*; Wilson, A. J. C., Ed.; Kluwer: Dordrecht, 1992; Vol. C.
44. Bruno, I. J.; Cole, J. C.; Edgington, P. R.; Kessler, M. K.; Macrae, C. F.; McCabe, P.; Pearson, J.; Taylor, R. *Acta Crystallogr., Sect. B* **2002**, *58*, 389–397.